Journal of Organometallic Chemistry 579 (1999) 24–29

Crystal structures and polymerization catalytic properties of 1,1,2,2-tetramethyldisilane-bis(3-*t*-butyl-η^5-cyclopentadienyl) titanium and zirconium dichlorides

Gonglu Tian, Baiquan Wang, Shansheng Xu, Yongqiang Zhang, Xiuzhong Zhou *

Department of Chemistry, Nankai University, Tianjin 300071, PR China

Received 24 November 1998; received in revised form 9 December 1998

Abstract

The title complexes $Me_4Si_2(1\text{-}C_5H_3\text{-}3\text{-}^tBu)_2MCl_2$ (M = Ti, **1**; M = Zr, **2**) have been prepared by reaction of $Li_2Me_4Si_2(C_5H_3\text{-}3\text{-}^tBu)_2$ with $MCl_4{\cdot}2THF$ in refluxing THF. *Rac*/*meso* ratio of about 2/3 was obtained for the titanocene complex **1**. But for the zirconocene **2**, only *meso* isomer was obtained. The crystal structures of *meso*-**1** and *meso*-**2** were determined. Their catalytic properties for ethylene polymerization have also been studied with MAO as a cocatalyst. © 1999 Elsevier Science S.A. All rights reserved.

Keywords: Titanium; Zirconium; Catalyst; Polymerization

1. Introduction

Ansa-metallocene derivatives of group 4 transition metals are of considerable current interest as catalysts for olefin polymerization [1,2]. It has been found that their catalytic properties have a close relationship with their structures, especially the ring-substituents and the bridge. In order to develop effective catalysts for olefin polymerization, considerable attention has been paid to complexes with Sila-bridged cyclopentadienyl and indenyl ligands [3–5]. Recently, we studied ethylene polymerization using tetramethyldisiloxane-bridged zirconocenes as catalysts and found that they showed some exciting results [6]. And if we use tetramethyldisilane-bridge instead of disiloxane-bridge, how about the catalytic properties? Based on our early work about tetramethyldisilane-bridged group 4 metallocenes [7–11], herein we report the synthesis, crystal structures and catalytic behavior of tetramethyldisilane-bridged metallocenes $Me_4Si_2(C_5H_3\text{-}3\text{-}^tBu)_2MCl_2$ (M = Ti, Zr).

2. Results and discussion

Complexes **1** and **2** were prepared by reaction $MCl_4{\cdot}2THF$ with $Li_2[Me_4Si_2(1\text{-}C_5H_3\text{-}3\text{-}^tBu)_2]$ in refluxing tetrahydrofuran (THF), according to Scheme 1.

The ^{1}H-NMR spectra of the reaction product revealed that both *racemic* and *meso* isomers had been formed for the titanocene complex **1**, with *rac*/*meso* ratio of about 2:3. Fractional crystallization from CH_2Cl_2/hexane allowed separation of the isomer pair of **1**. The *meso* isomer was identified by crystal structure determination. But for the zirconocene complex **2**, only *meso* isomer had been obtained. It seems that *meso* isomer instead of the *rac* isomers are most favored sterically for tetramethyldisilane-bridged metallocenes. Interestingly, Brintzinger and coworkers have reported the preparation of tetramethylethanediyl- and dimethylsilyl-bridged analogues. In their studies, the

---

* Corresponding author. Tel.: +86-22-23504781; fax: +86-22-23502458.

E-mail address: zhouxz@public1.tpt.tj.cn (X. Zhou)

PII: S0022-328X(98)01174-7

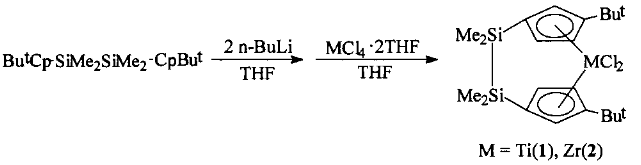

Scheme 1.

amount of *rac* isomers equals or exceeds that of *meso* isomer [12].

The ^{1}H-NMR spectra of complexes **1** and **2** agree with the composition of the complexes. Two SiMe$_2$ proton signals are apparent for **1** and **2** in solution. The two SiMe$_2$ proton signals for *rac*- and *meso*-**1** are almost identical, one at 0.42 ppm and the other at 0.35(6) ppm. Three signals at 6.2–7.0 ppm can be assigned to the cyclopentadienyl protons, which shift toward low-fields compared with the teramethylethanediyl-bridged analogues [12].

The crystallographic X-ray analysis of a cube-shaped crystal grown from a concentrated solution of **1** in CH_2Cl_2/hexane confirms the presence of the *meso* isomer *meso*-**1** only. Data of particular relevance for the X-ray study are given in Table 1. Figs. 1 and 2 present two alternative views of the molecular structure of *meso*-**1**, and Table 1 presents some selected bond distances and bond angles, respectively. The structure of *meso*-**1** shows the expected planar symmetry, the molecular symmetry plane coinciding with the Cl–Ti–Cl plane. In contrast, its tetramethylethanediyl-bridged analogue shows an asymmetric arrangement [12]. The two five-membered ring ligands of *meso*-**1** are overlapped. The *t*-butyl group locates in one of the β-positions relative to the bridge-head atom, lying just above or below one of the chlorine atom due to the presence of the bulky *t*-butyl substituents. Some structural parameters of *meso*-**1** (e.g. the Ti–centroid distance of 2.115 Å, the centroid–Ti–centroid angle of 134.7 (and the Cl–Ti–Cl angle of 97.9°) are somewhat different from those (2.065 Å, 132.6° and 94.77°, respectively) for the unsubstituted complex $Me_4Si_2(C_5H_4)_2TiCl_2$ [7].

Table 1
Selected bond lengths (Å) and angles (°) for *meso*-**1** [a]

Ti(1)–Cl(1)	2.349 (2)	Si(1)–C(11)	1.874 (5)
Ti(1)–Cl(2)	2.347 (2)	Si(1)–Si(1a)	2.324 (3)
Ti(1)–C(11)	2.375 (4)	C(11)–C(12)	1.429 (7)
Ti(1)–C(12)	2.347 (4)	C(11)–C(15)	1.428 (6)
Ti(1)–C(13)	2.431 (5)	C(12)–C(13)	1.403 (6)
Ti(1)–C(14)	2.548 (5)	C(13)–C(14)	1.411 (6)
Ti(1)–C(15)	2.457 (5)	C(14)–C(15)	1.422 (7)
Ti(1)–CEN	2.115	C(14)–C(20)	1.515 (6)
C(11)–Si(1)–Si(1a)	103.1(1)		
Cl(1)–Ti(1)–Cl(2)	97.9(1)		
PL(1)–PL(2)	124.3(1)		
CEN(1)–Ti(1)–CEN(2)	134.7		

[a] PL, The plane of five-membered ring. CEN, The center of five-membered ring.

The molecular structure of complex *meso*-**2**, represented in Figs. 3 and 4, shows a similar planar symmetry, selected bond distances and bond angles are listed in Table 2.

Complexes **1** and **2** were employed as catalysts for ethylene polymerization, with MAO as a cocatalyst. Polymerization was conducted in toluene solution under 1 atm monomer pressure. The results are listed in Table 3.

As we can see from Table 3, complex **1** only shows very low activity for ethylene polymerization. On the other hand, complex **2** shows considerable activity (2.09 × 10^6 g PE/mol Zr h at 30°C), it approaches the

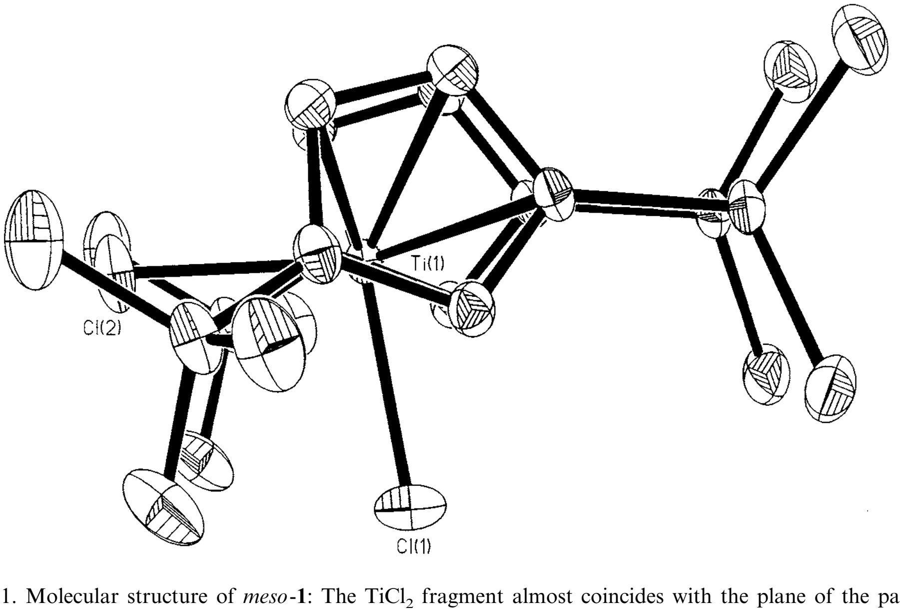

Fig. 1. Molecular structure of *meso*-**1**: The $TiCl_2$ fragment almost coincides with the plane of the paper.

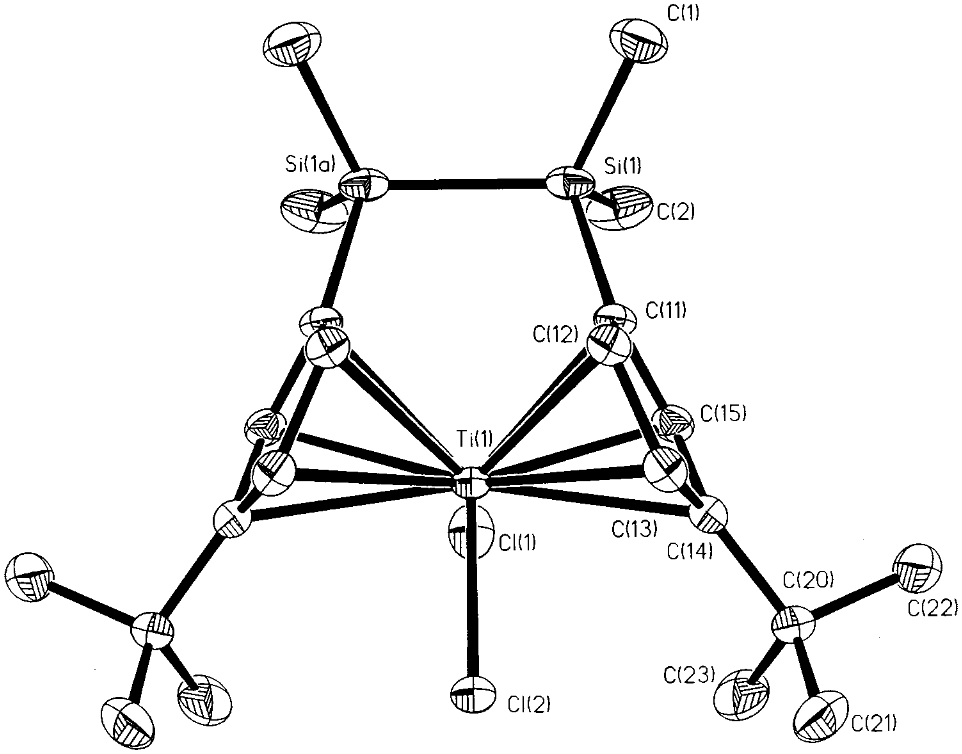

Fig. 2. Molecular structure of *meso*-**1**: The $TiCl_2$ fragment is oriented almost perpendicular to the plane of the paper.

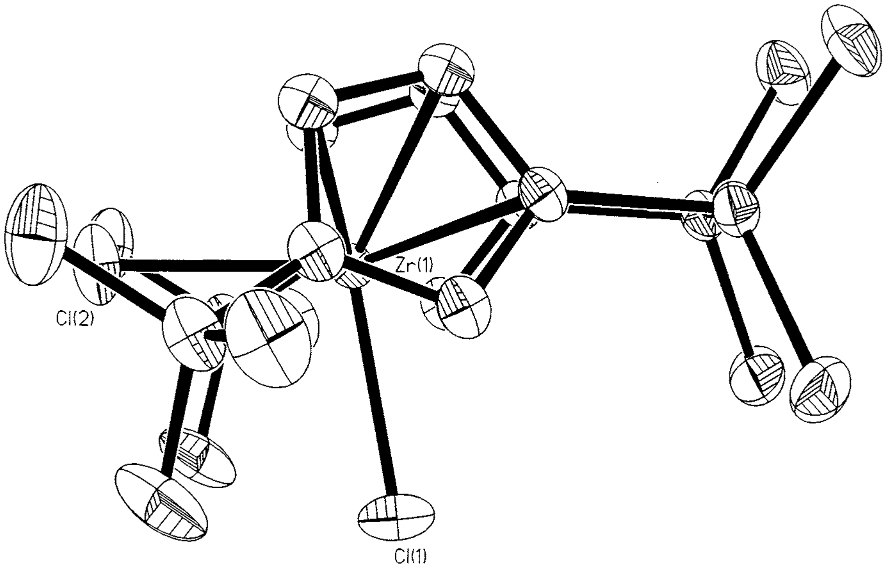

Fig. 3. Molecular structure of *meso*-**2**: The $ZrCl_2$ fragment almost coincides with the plane of the paper.

activity of Cp_2ZrCl_2 (4.35×10^6 g PE/mol Zr h at 40°C). But the molecular weight of polyethylene obtained is still very low and the activity decreases as the temperature increases. The presence of bulky *t*-butyl substituents may be responsible for the low activities of **1** and the low molecular weight of polyethylene producing with **2**. We can see from Figs. 1 and 2 that the *t*-butyl group lies just above one of the M–Cl bonds, which are active sites in the catalytic reaction. The presence of *t*-butyl group prevents monomer from coordinating with the central metal and inserting into the M–R bond. As a result, complex **1** shows low activities for ethylene polymerization. Because of the larger atom radius of zirconium than that of titanium, complex **2** has less steric effect than complex **1** and has higher activity for ethylene polymerization, but the molecular weight of polyethylene obtained is still very low due to the steric effect. From Table 3 it is also found that the

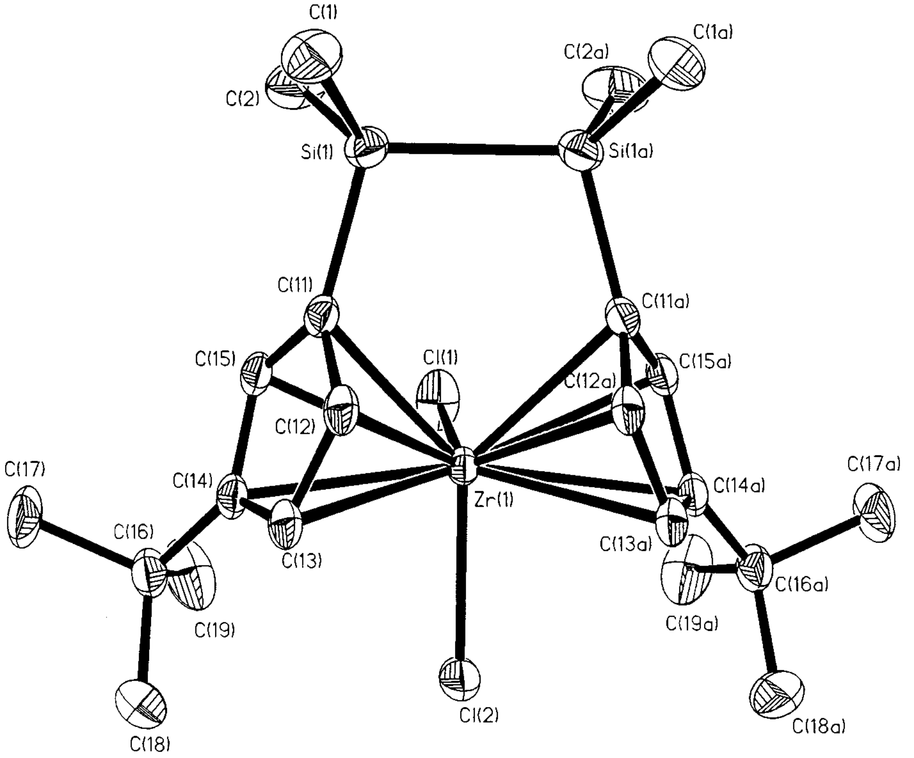

Fig. 4. Molecular structure of *meso*-**2**: The $ZrCl_2$ fragment is oriented almost perpendicular to the plane of the paper.

activities decrease with increasing temperature which seems somewhat strange compared to other reports. It is attributed probably to the less stability of *meso*-**2** in higher temperature due to the steric effect. If we further decrease the polymerization temperature, the activity should decrease. Tetramethyldisiloxane-bridged analogue *rac*-$(Me_2SiOSiMe_2)(1\text{-}C_5H_3\text{-}3\text{-}^{t}Bu)_2ZrCl_2$ also shows the highest activity at lower temperature (40°C) than the other zirconocenes [6].

3. Experimental

All operations were carried out under an argon atmosphere using standard Schlenk techniques. Toluene and tetrahydrofuran were purified by refluxing over sodium/$(C_6H_5)_2CO$ system under argon. Polymerization grade ethylene (Yanshan Petrochemicals, China) was used without further purification. ^{1}H-NMR spectra were recorded on Bruker AC-200 spectrometer and MS spectra on VG-7070E HF. Elemental analyses were carried out at the CHN Corder MF-3 Elemental Analysis Facility. Details of the single-crystal X-ray study are collected in Table 4. $^{t}BuCpSiMe_2SiMe_2Cp^{t}Bu$ [13], $TiCl_4 \cdot 2THF$ and $ZrCl_4 \cdot 2THF$ [14] were prepared according to literature.

Table 2
Selected bond lengths (Å) and angles (°) for *meso*-**2**

Zr(1)–Cl(1)	2.441 (2)	Si(1)–C(11)	1.882 (6)
Zr(1)–Cl(2)	2.433 (3)	Si(1)–Si(1a)	2.331 (3)
Zr(1)–C(11)	2.481 (5)	C(11)–C(12)	1.432 (9)
Zr(1)–C(12)	2.466 (5)	C(11)–C(15)	1.425 (7)
Zr(1)–C(13)	2.549 (6)	C(12)–C(13)	1.415 (8)
Zr(1)–C(14)	2.630 (5)	C(13)–C(14)	1.421 (8)
Zr(1)–C(15)	2.559 (5)	C(14)–C(15)	1.423 (9)
Zr(1)–CEN	2.238	C(14)–C(16)	1.527 (8)
Cl(1)–Zr(1)–Cl(2)	100.6(1)	C(11)–Si(1)–Si(1a)	105.0(2)
PL(1)–PL(2)	123.0(1)	CEN(1)–Zr(1)–CEN(2)	131.5

Table 3
Results of ethylene polymerization catalyzed with **1** and **2**/MAO [a]

Catalyst	Tp (°C)	Yield (g)	A (kgPE/ mmol Zr h)	Mη ($\times 10^{-4}$) (g mol^{-1})
meso-**1**	20	Trace	Very low	–
	40	trace	Very low	–
meso-**2**	30	3.13	2.09	7.07
	40	2.69	1.79	5.67
	60	2.10	1.40	4.41
Cp_2ZrCl_2	40	6.52	4.35	44.8

[a] Polymerization conditions: $[M] = 3.0 \times 10^{-6}$ mol, Al/Zr = 2500, $t = 30$ min, 1 atm of monomer pressure, in 100 ml toluene.

Table 4
Summary of X-ray diffraction data of *meso*-**1** and *meso*-**2**

	meso-**1**	*meso*-**2**
Formula	$C_{22}H_{36}Cl_2Si_2Ti$	$C_{22}H_{36}Cl_2Si_2Zr$
Formula weight	475.51	518.03
Space group	$P2_1/m$ (#11)	$P2_1/m$ (#11)
Crystal system	Monoclinic	Monoclinic
Z	2	2
a (Å)	6.881(1)	6.921(1)
b (Å)	19.026(4)	19.304(4)
c (Å)	10.039(2)	10.024(2)
α (°)	90.00(0)	90.00(0)
β (°)	102.81(3)	103.80(3)
γ (°)	90.00(0)	90.00(0)
Volume (Å^3)	1283(1)	1301(1)
$D_{calc.}$ (g cm^{-3})	1.231	1.325
Crystal size (mm)	$0.20\times0.30\times0.70$	$0.30\times0.30\times0.40$
Radiation (Å^3)	Mo–K$_\alpha$ ($\lambda = 0.71069$)	Mo–K$_\alpha$ ($\lambda = 0.71069$)
μ (mm^{-1})	0.6371	7.191
Data collection method	$\omega/2\theta$	$\omega/2\theta$
Max 2θ (°)	46	46
Total no. of observations	1969	1993
No. of unique data, $I>3\sigma(I)$	1515	1693
Final no. of variables	127	127
R	0.040	0.042
R_w	0.051	0.053
Goodness-of-fit	1.27	1.61

3.1. Preparation of tetramethyldisilane-bridged bis(t-butylcyclopentadienyl) titanium dichlorides (*1*)

To a solution of 2.22 g (6.2 mmol) of ${}^t\mathrm{BuCpSiMe_2SiMe_2Cp}{}^t\mathrm{Bu}$ in 50 ml of THF cooled down to 0°C (ice bath), 6.2 ml (12.4 mmol, 2.0 N in hexane) of *n*-BuLi was added dropwise. After stirring at ambient temperature for 6 h, the resulting yellowed solution was transferred via a cannula to a refluxing solution of 2.07 g (6.2 mmol) of $TiCl_4 \cdot 2THF$ in ca. 30 ml of THF. The resulting suspension was maintained refluxing for 18 h. After solvent evaporation and uptake of the residue in 30 ml of CH_2Cl_2, the resulting suspension was filtered through a Al_2O_3 pad. The filtrate was evaporated to dryness. The residue was dissolved in ca. 10 ml Et_2O, and stored at −20°C for several days. The crude product was obtained as microcrystalline, deep red solid (yield 0.63 g). The ^{1}H-NMR spectrum showed the signals of both isomers in a *rac*/*meso* ratio of about 2:3. Recrystallization of the crude product mixture from CH_2Cl_2/*n*-hexane gave 0.18 g of *meso*-**1** as deep-red cube-shaped crystal. The mother liquid was concentrated and the solid obtained was recrystallized from CH_2Cl_2/*n*-hexane for several times. The pure isomer *rac*-**1** was obtained as deep-red needle crystals (yield 0.14 g). *meso*-**1**. M.p. 215–216°C. Anal. Found: C, 55.80; H, 7.76. $C_{22}H_{36}Cl_2Si_2Ti$ Calc.: C, 55.57; H, 7.63. ^{1}H-NMR ($CDCl_3$): δ 6.74 (br, 2H, C_5H_3), 6.63 (br, 2H, C_5H_3), 6.27 (br, 2H, C_5H_3), 1.37 (s, 18H, $C(CH_3)_3$), 0.42 (s, 6H, Si–CH_3), 0.36 (s, 6H, Si–CH_3). MS (*m*/*e*,% intensity): 474 (100, M$^+$), 438 (9, [M–HCl]$^+$), 417 (11, [M–C_3H_7]$^+$), 366 (18, [M–Me_3SiCl]$^+$), 346 (6, [M–Me_2SiCl_2]$^+$), 330 (15, [M–HCl–Me_3SiCl]$^+$), 163 (45, [$\mathrm{Cp}^t\mathrm{BuSiMe}$]$^+$), 73 (73, Me_3Si^+). *rac*-**1**: M.p. 213–215°C, ^{1}H-NMR ($CDCl_3$): δ 6.96 (m, 2H, C_5H_3), 6.76 (t, 2H, C_5H_3), 6.43 (m, 2H, C_5H_3), 1.30 (s, 18H, $C(CH_3)_3$), 0.42 (s, 6H, Si–CH_3), 0.36 (s, 6H, Si–CH_3).

3.2. Preparation of tetramethyldisilane-bridged bis(t-butylcyclopentadienyl) zirconium dichlorides (*2*)

An analogous procedure gave the zirconocene *meso*-**2** in a yield of 11%. No *rac*-**2** signals were observed in the ^{1}H-NMR spectrum of the crude product. M.p. 188–190°C. Anal. Found: C, 50.70; H, 7.67. $C_{22}H_{36}Cl_2Si_2Zr$ Calc.: C, 50.93; H, 6.99. ^{1}H-NMR ($CDCl_3$): (6.65 (t, 2H, C_5H_3), 6.57 (t, 2H, C_5H_3), 6.43 (t, 2H, C_5H_3), 1.30 (s, 18H, $C(CH_3)_3$), 0.43 (s, 6H, Si–CH_3), 0.36 (s, 6H, Si–CH_3). MS (*m*/*e* % intensity): 516 (100, M$^+$), 481 (4, [M–Cl]$^+$), 445 (7, [M–Cl–HCl]$^+$), 423 (69, [M–Cl–Me_2Si]$^+$), 407 (18, [M–HCl–Me_3Si]$^+$), 371 (9, [M–Me_3Si-2 HCl]$^+$), 163 (29, [$\mathrm{Cp}^t\mathrm{BuSiMe}$]$^+$), 73 (31, Me_3Si^+).

3.3. X-ray crystallography of meso-*1* and meso-*2*

A summary of the crystallographic results is presented in Table 4. Crystals of **1** and **2** suitable for X-ray diffraction obtained from CH_2Cl_2/hexane solution. All data sets were collected on an Enraf–Nonius CAD-4 diffractometer with graphite monochromated Mo–K$_\alpha$ radiation. The empirical absorption correction using the program DIFBAS was applied for **1** and **2**. All calculations for **1** and **2** were performed on PDP11/44 and IBM 486 computers using the SDP-PLUS program system. The structures of **1** and **2** were solved by direct methods and expanded using Fourier techniques. The non-hydrogen atoms were refined anisotropically. Hydrogen atoms were not included in the refinement and calculations of structure factors. Neutral atom scattering factors were taken from the tabulation of Cromer and Wabe.

3.4. Ethylene polymerization

Polymerization was carried out in a 250 ml glass reactor with a magnetic stirring bar at about 780 mmHg. Toluene (100 ml) was introduced into the reactor, the temperature was increased to polymerization temperature, and then toluene was saturated with ethylene. A prescribed amount of MAO and a given metallocene dissolved in toluene were injected into the reactor to initiate the polymerization.

Acknowledgements

We are grateful to the National Science Foundation of China, Petro-Chemical Corporation, State Commission of Science and Technology of China and the 21st Century Youth Science Foundation of Tianjin for financial support of this work.

References

[1] H.H. Brintzinger, D. Fischer, R. Mulhaupt, B. Rieger, R.M. Waymouth, Angew. Chem. Int. Ed. Engl. 34 (1995) 1143.

[2] W. Kaminsky, M. Arndt, Adv. Polym. Sci. 127 (1997) 143.

[3] P.C. Mohring, N.J. Coville, J. Organomet. Chem. 479 (1994) 1.

[4] W. Spaleck, F. Kuber, A. Winter, J. Rohrmann, B. Bachmann, M. Antberg, V. Dolle, E.F. Paulus, Organometallics 13 (1994) 954.

[5] W. Spaleck, M. Antberg, V. Dolle, R. Klein, J. Rohrmann, A. Winter, New J. Chem. 14 (1990) 499.

[6] B. Wang, L. Su, S. Xu, R. Feng, X. Zhou, D. He, Macromol. Chem. Phys. 198 (1997) 3197.

[7] Y. Wang, S. Xu, X. Zhou, R. Wang, X. Yao, Acta Chim. Sinica 46 (1988) 674.

[8] X. Zhou, Y. Wang, S. Xu, H. Wang, R. Wang, Sci. China (B) 34 (1991) 1048.

[9] Y. Wang, X. Zhou, X. Yao, H. Wang, Gaodeng Xuexiao Huaxue Xuebao 12 (1991) 488.

[10] Y Wang, X. Zhou, Youji Huaxue 12 (1992) 286.

[11] X. Zhou, Y. Wang, S. Xu, H. Wang, X. Yao, Chem. Res. Chinese Univ. 8 (1992) 239.

[12] S. Gutmann, P. Burger, H.H. Hund, J. Hofmann, H.H. Brintzinger, J. Organomet. Chem. 369 (1989) 343.

[13] X. Zhou, Y. Zhang, W. Xie, S. Xu, J. Sun, Organometallics 16 (1997) 3474.

[14] L. Manzer, Inorg. Synth. 21 (1982) 135.